The influence of topography on the development of hail storms near to the Andes mountains

Alejandro de la Torre
Austral University
and
CONICET
(National Scientific and Technical Research Council)
Buenos Aires, Argentina
(adelatorre@austral.edu.ar)

Preliminar comments:

- **The comprehension of the atmospheric circulation is essential to understand the interaction among different spatial and temporal scales**

- **Meteorological phenomena over complex terrain: rugosity changes the atmospheric height at each location, giving place to different vertical tropospheric structures along a given region.**

- **Sawyer (1956): the hills intensify precipitation over rain areas already determined by dynamical factors.**

- **Smith (1979): one of the ways in which orography influences the weather is by controlling the rainfall distribution.**

- Houze (2012): orographic precipitation is not caused by topography but, occurs when storms of a type that can take place anywhere (deep convection, fronts, tropical cyclones) form near or move over complex terrain

- The effects of topography on air motion operate over a wide range of scales, from planetary-scale wave motion to micro-scale wave motion through turbulence and mixing (Fritts and Alexander, 2003)

- The impact that the Andes Range produces on the movements of air masses and precipitation

- Kleeman (1989): the implication of the circulation process over the Amazon basin and high Andean plateau, using numerical model simulations

- Garreud (1999): the alternation of dry and rainy episodes over the bolivian Antiplano, due to the orography

- **Saurral et al. (2014): the impact of varying artificially the altitude of the Andes Cordillera in global climate models and the increase of the model horizontal resolution. How these variations determine moisture fluxes and precipitation over some regions of South America? big influence of the location and shape of Andes in the climatology**

- **Different processes related to the Andes and west-east relief gradient influence the generation of mesoscale circulations that may be affected by surface friction and large-scale pressure gradients, forcing deep moist convection (Nicolini and García Skabar, 2011)**

- **These mesoscale circulations are associated with divergence/convergence patterns in the boundary layer over the plains or over complex terrain (Pan et al., 2004, Barthlott et al., 2006, 2010, Kalthoff et al., 2009)**

- **The comprehension of the variability of the influx of water vapour (WV) over the argentinean Cuyo region (Mendoza) is of major importance**

- **It could be mostly induced by the southward movement of the Chaco LLJ (Low Level Jet) from northern Argentina (Nicolini and Saulo, 2000, Salio et al., 2002) or from Uruguay, southeast Brazil and the Atlantic Ocean**

- **Nevertheless, in some cases, after crossing the Andean mountains, the South Pacific anticyclone can deplete or suppress the presence of LLJ with a consequent temperature and humidity decrease (Wang and Fu, 2004)…. after the anticyclone arrives at the Atlantic coasts, the temperature may increase again and deep convection may reappear over the Mendoza region**

From 2 recent contributions:

1. **Trigger of hail storms by mountain waves**

2. **Detection of humidity accumulation as well as its distribution, from GNSS ground receivers**

1

(de la Torre et al., Atmos. Res., doi: 10.1016/j.atmosres.2014.12.020156, 2015)

- **The atmosphere to the east of the Andes, between the polar and subtropical jets is a natural laboratory for the formation of mountain gravity waves (i.e. Eckermann and Preusse, 1999, Nature; de la Torre et al, 2006, GRL)**

- **In the semiarid region of Mendoza, between latitudes 32S and 36S, all known sources of gravity waves occur permanently**

- **The valleys are a frequent scene for the occurrence of strong convection processes with production of hail**

3 ingredients for a good storm are needed:

- **unstable conditions,**
- **humidity convergence,**
- **and a trigger element constituted by one or more mechanisms. Then,**
- **moist air is pushed upward (or pumped) from near the surface to higher levels of free convection**

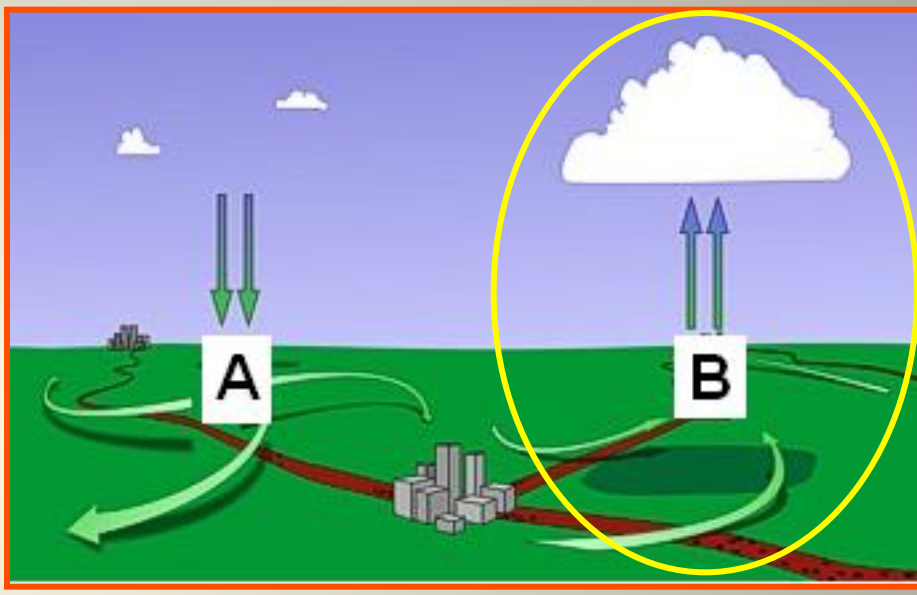

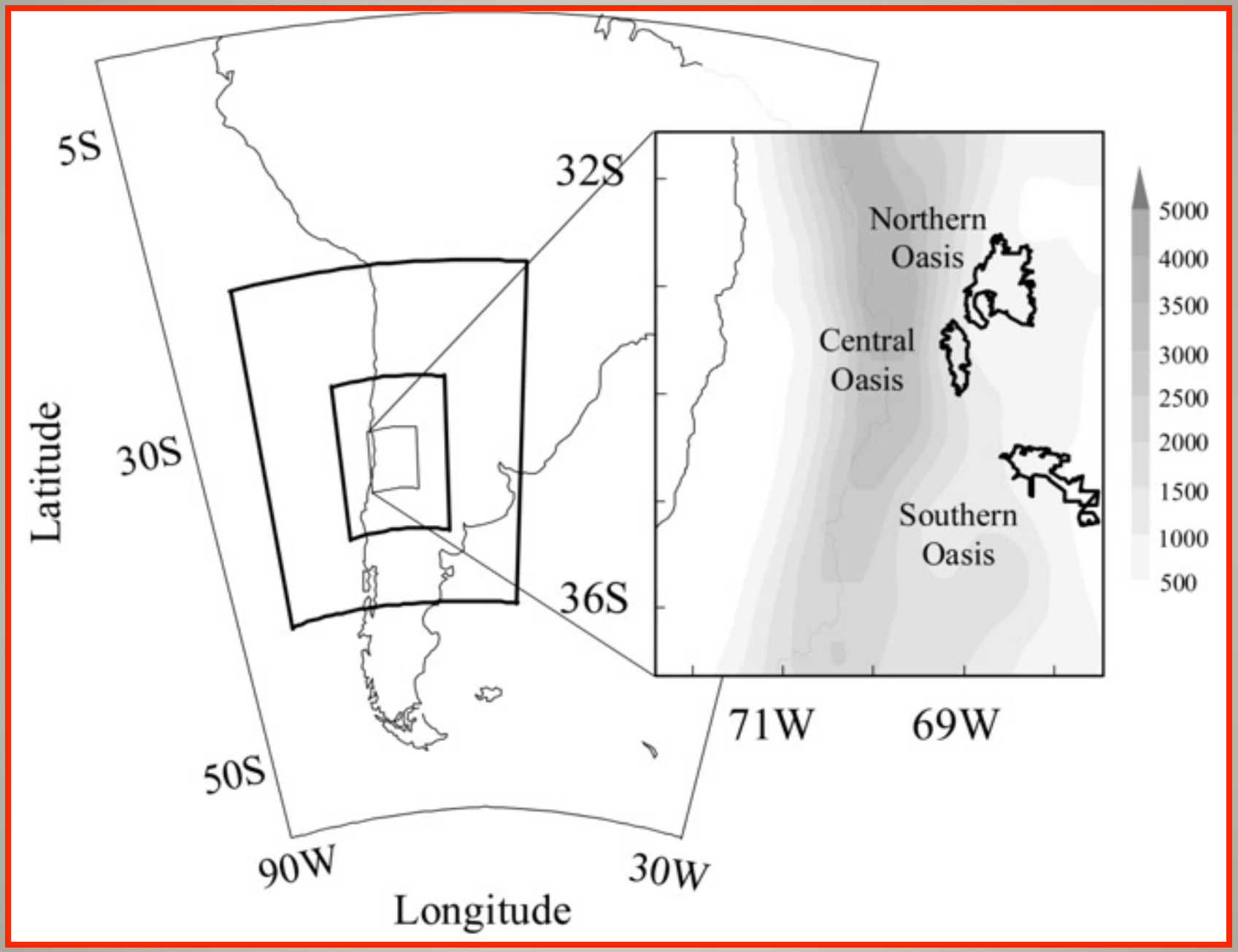
5S
30S
50S
Latitude
90W
30W
Longitude
32S
36S
71W
69W
Northern Oasis
Central Oasis
Southern Oasis
5000
4000
3500
3000
2500
2000
1500
1000
500

An Operational Program for Hail Suppression in the Province of Mendoza (Argentina)

1. 4 Aircrafts
2. 4 S-Band MRL-5 Radars
3. Authomatic ground based silver iodide generators
4. Hail pad network
5. Mesoscale models to forecast deep convection

www.contingencias.mendoza.gov.ar

Contact & info: adelatorre@austral.edu.ar

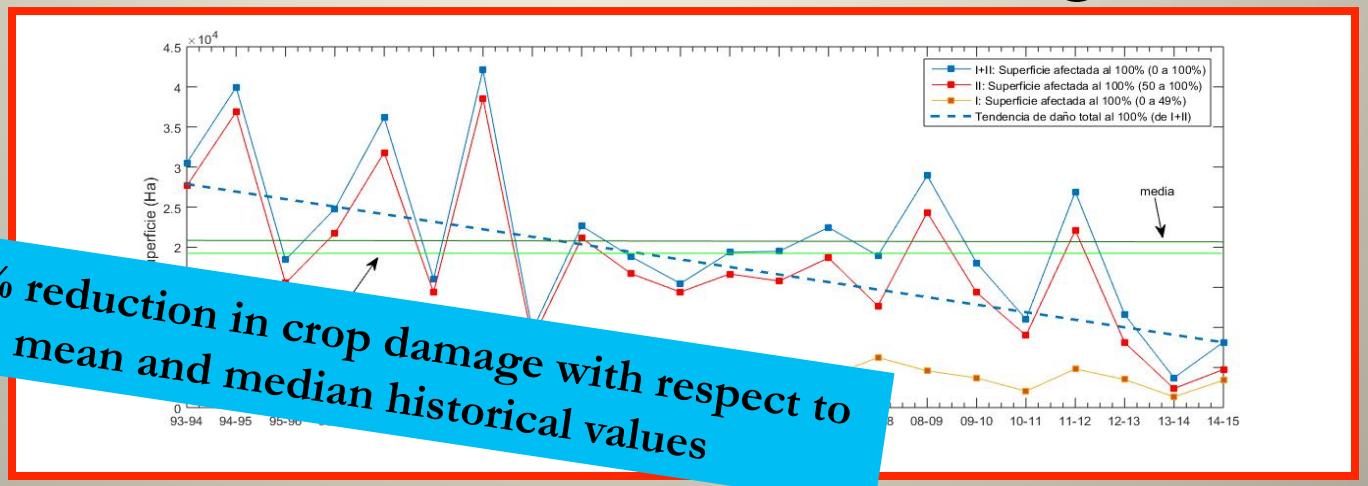

A 50% reduction in crop damage with respect to mean and median historical values

The usual trigger elements of severe storms at Mendoza are:

1. Cold fronts

2. Anabatic and katabatic winds within the valleys

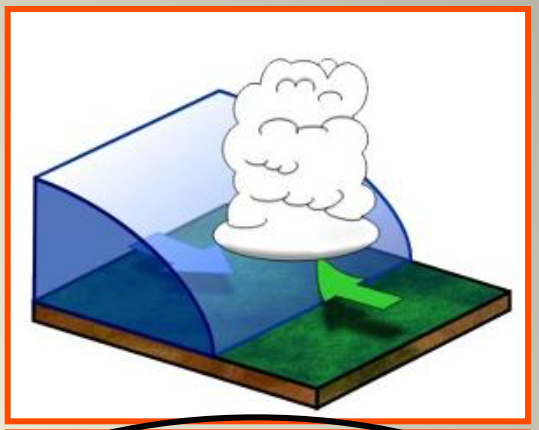

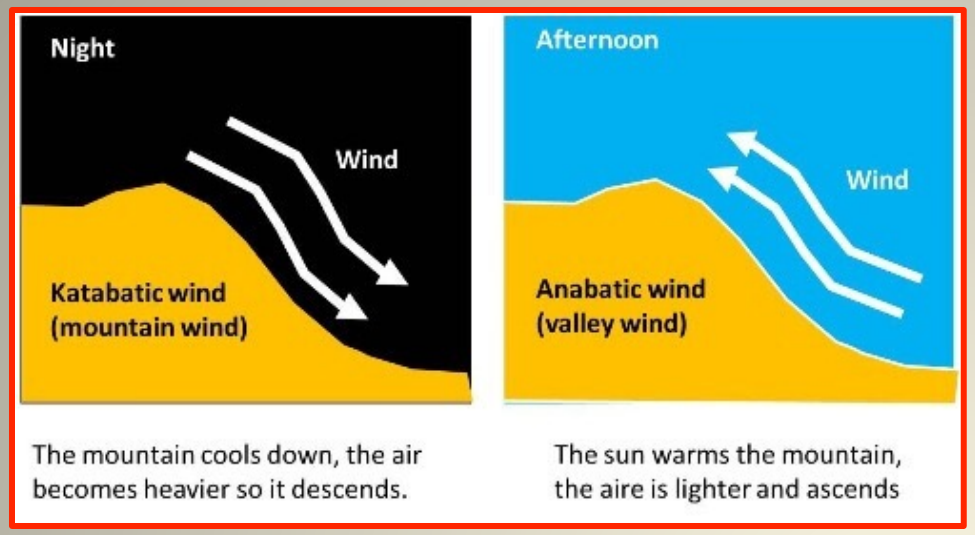

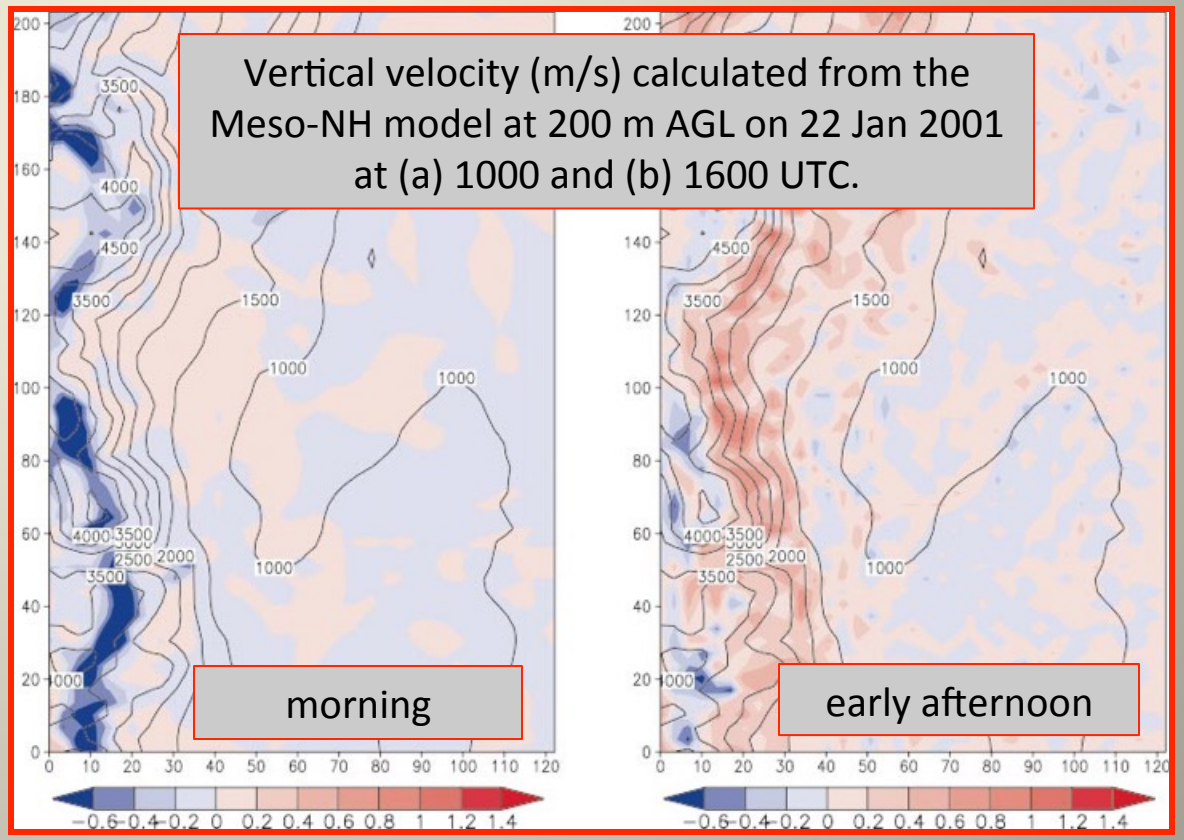

(de la Torre et al. Mon Wea Rev, 132, 9, 2259-2268, 2004)

Usual triggering elements of severe storms at Mendoza:

1. Cold fronts

2. Anabatic and katabatic winds within the valleys

3. <u>Mountain gravity waves (MWs)</u>

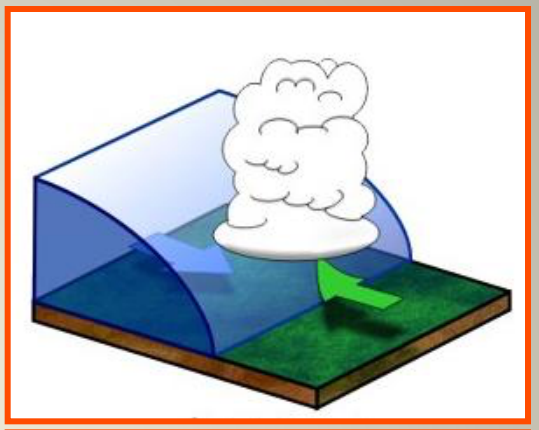

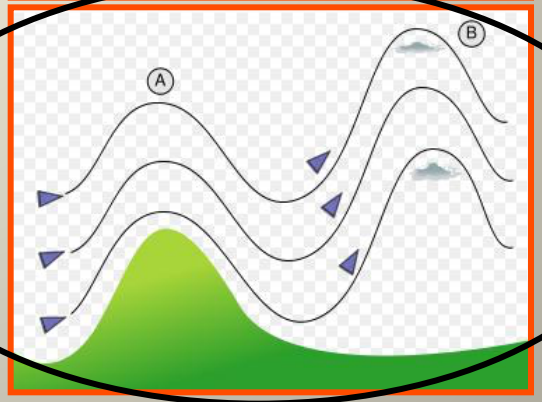

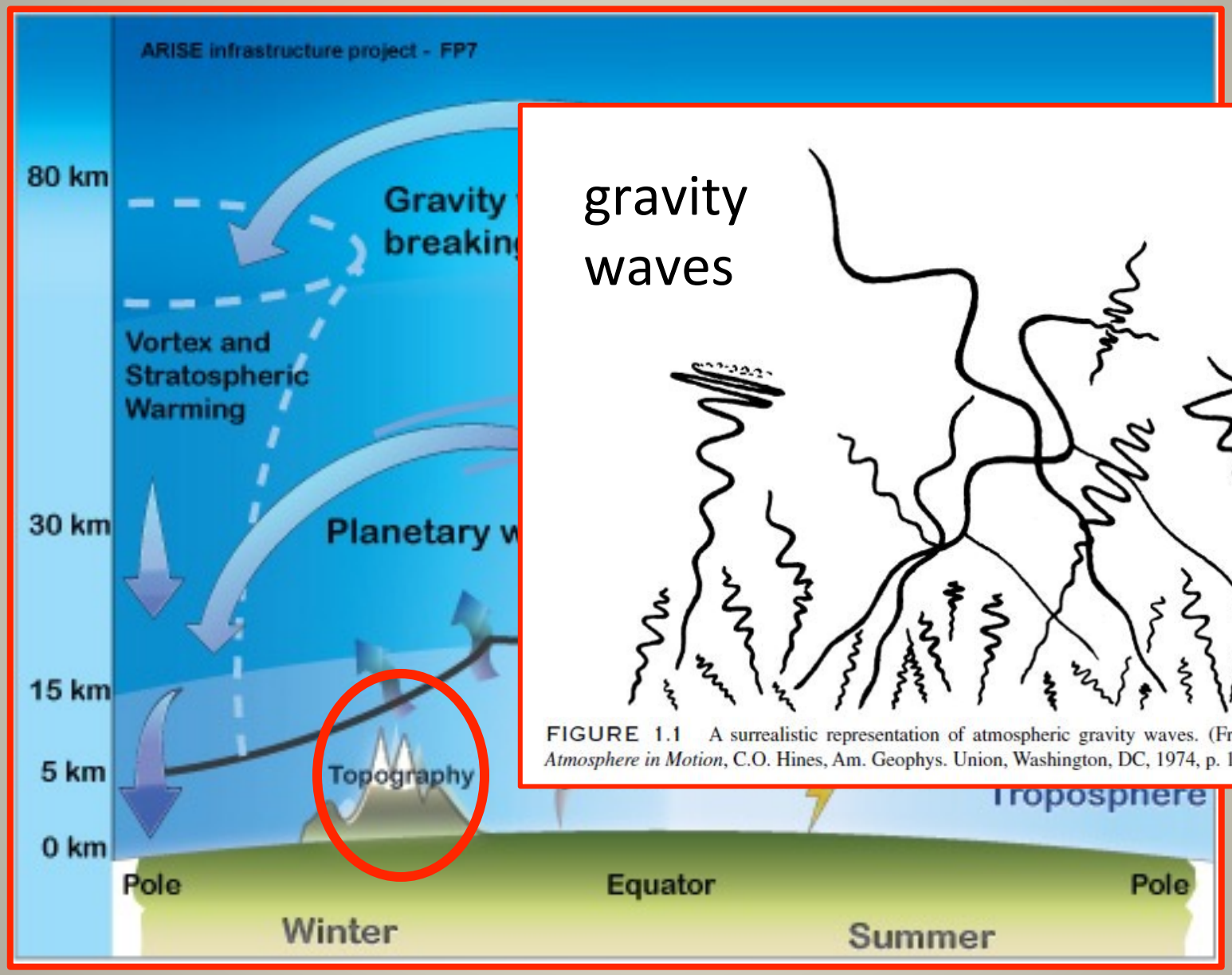

gravity waves

FIGURE 1.1 A surrealistic representation of atmospheric gravity waves. (From *The Upper Atmosphere in Motion*, C.O. Hines, Am. Geophys. Union, Washington, DC, 1974, p. 194.)

Mountain waves are a subfamily from

Gravity Waves

A stable atmosphere, under uniform stratification conditions:

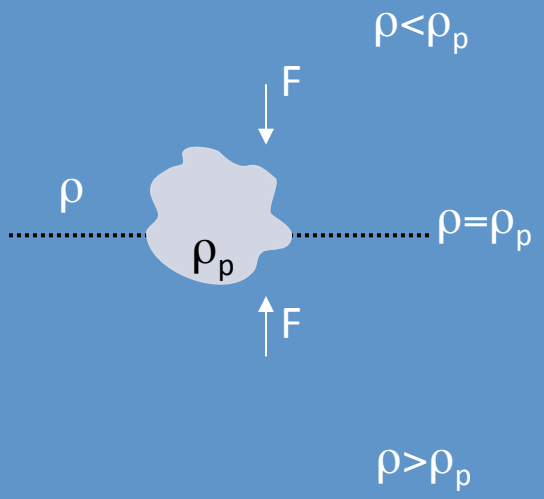

$$\frac{d^2 z_p}{dt^2} = \left(\frac{\rho - \rho_p}{\rho_p} \right) g = F$$

- GWs are transversal waves that represent the principal mechanism in the atmosphere able to transport energy and momentum between different altitudes and geographic regions

- Principal sources of GWs are:
  - Orographic forcing
  - Deep convection and fronts
  - Shear instability
  - Geostrophic adjustment

Basic equations:

$\vec{v} = (u_0+u', v_0+v', 0+w')$

$$\frac{\partial u'}{\partial t} - fv' = -\frac{1}{\rho_0}\frac{\partial p'}{\partial x}$$

$$\frac{\partial v'}{\partial t} + fu' = -\frac{1}{\rho_0}\frac{\partial p'}{\partial y}$$

$$\frac{\partial w'}{\partial t} = -\frac{1}{\rho_0}\frac{\partial p'}{\partial z} - \frac{\rho}{\rho_0} g$$

$$\frac{\partial u'}{\partial x} + \frac{\partial v'}{\partial y} + \frac{\partial w'}{\partial z} = 0$$

$$\frac{\partial \rho'}{\partial t} + w' \frac{\partial \rho_0}{\partial z} = 0$$

Linearized momentum and mass equations

$$w = w_0 \exp(kx + ly + mz - \omega t)$$

$$\vec{k} = (k, l, m)$$

$$\omega^2 = \frac{f^2 m^2 + N^2 (k^2 + l^2)}{k^2 + l^2 + m^2}$$

$$E = \frac{1}{2}\rho\,\overline{(u'^2 + v'^2 + w'^2)} + \frac{1}{2}\overline{\left(\frac{g}{N}\right)^2 \left(\frac{T'}{T_f}\right)^2}$$

$$\frac{\text{Kinetic energy}}{\text{Potential energy}} = 1 + \frac{2f^2}{N^2}\,\mathrm{tg}^2 j'$$

Three ranges may be distinguished

- Non hydrostatic $w \leq N$
- Hydrostatic non rotating $f << w << N$
- Hydrostatic rotating $w \geq f$

$f = 2W \,\mathrm{sen}(lat)$

All the dynamic and thermodynamic variables are related within any GW through the polarization relations

- In the non hydrostatic range, *u'* and *v'* are linearly polarized
- With rotation, *u'* and *v'* are elliptically polarized

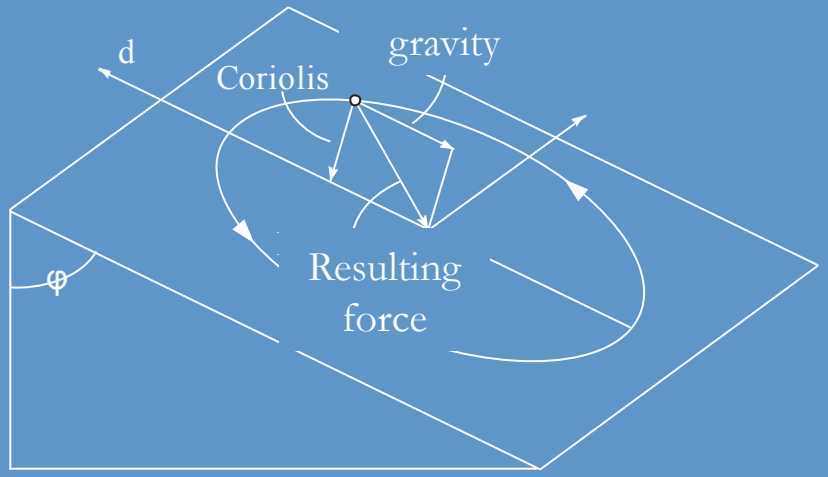

- From a total of 180 storms between 2004 and 2011, we consider here 15 of them where intense MWs and no cold fronts where detected
- 120 in northern and central crop areas (oases)
- differences with 60 storms in the southern oasis (Hierro et al, Atmos Res, 2013)
- effects of flow over topography favoring deep convection
- joint occurrence of storms + hail + MWs is determined from WRF, radar and RS
- two case studies
- simulations are validated with RS data
- the necessary energy to lift a parcel to its level of free convection is tested from CAPE and CIN, then
- CIN is compared against the MWs' $(1/2)w^2$
- MWs amplitude are able to provide the necessary energy to lift the air parcel and trigger convection
- Conceptual scheme

Genesis of severe storms - First Radar Echoes (FRE)

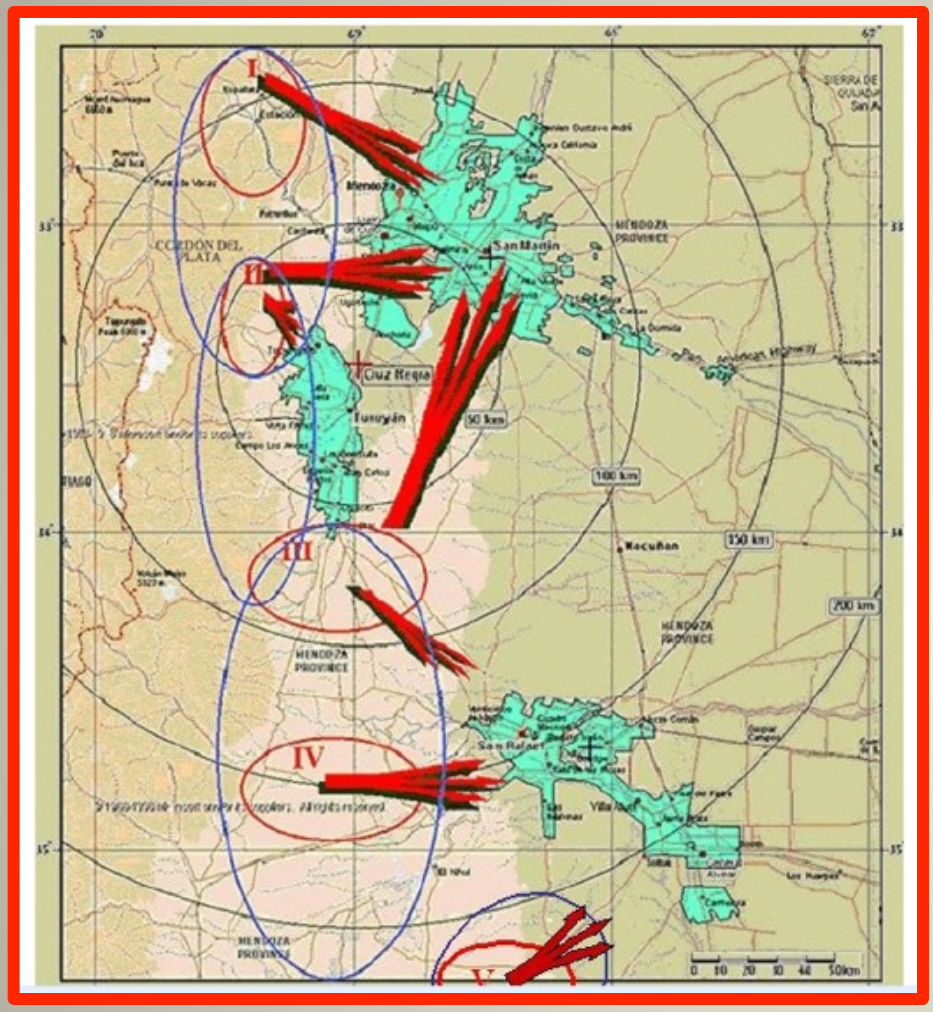

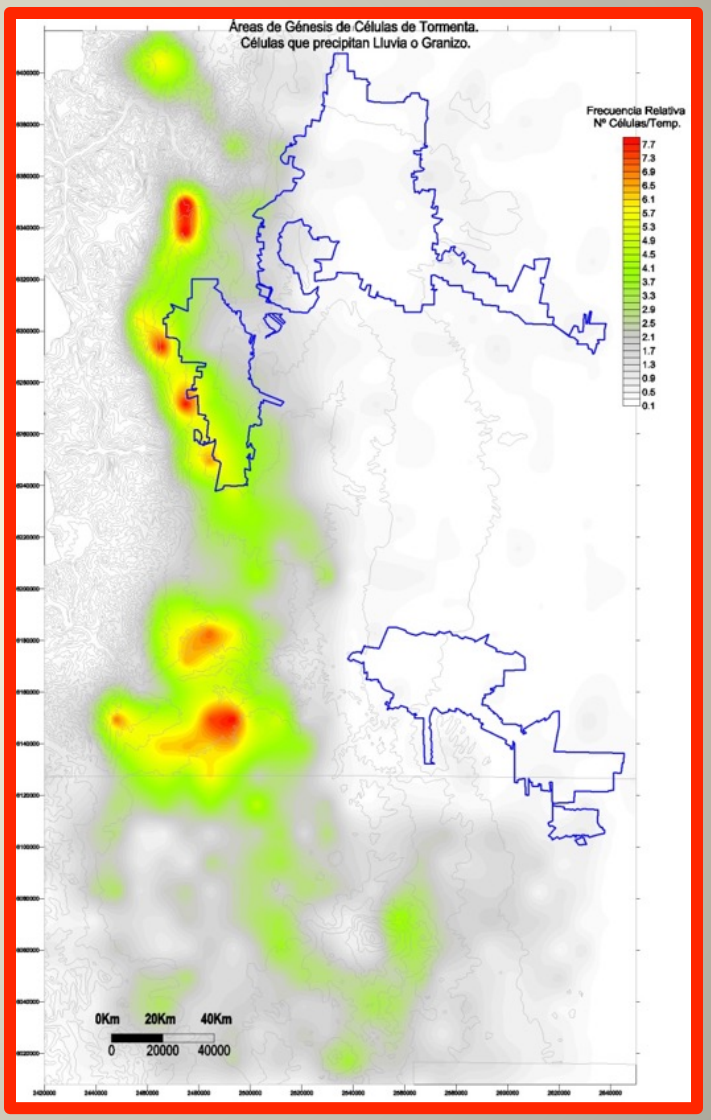

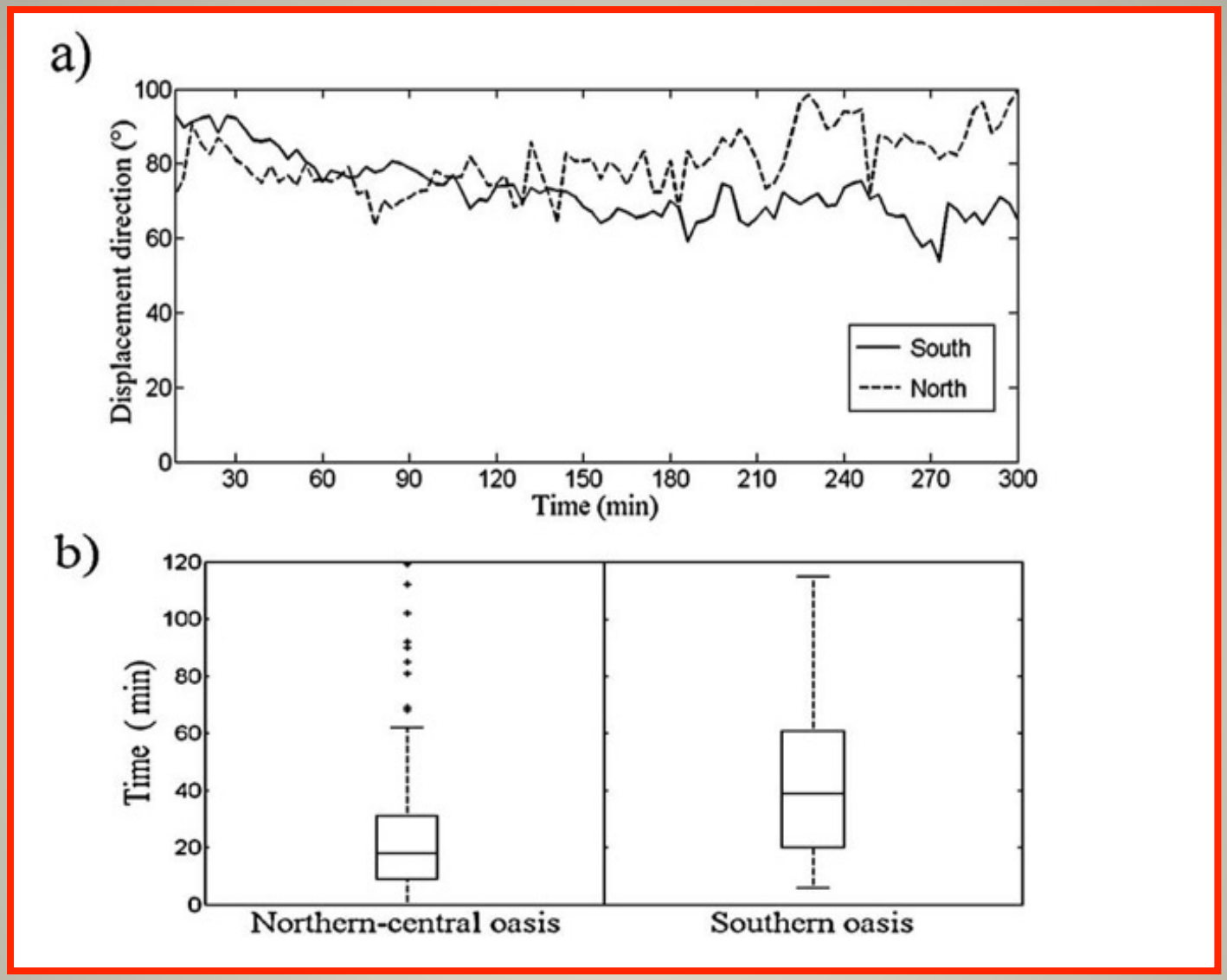

a) Mean displacement direction, 226 and 228 storm cells, 2004-2011

b) Time required by every storm cell to reach hail threshold parameters in both regions

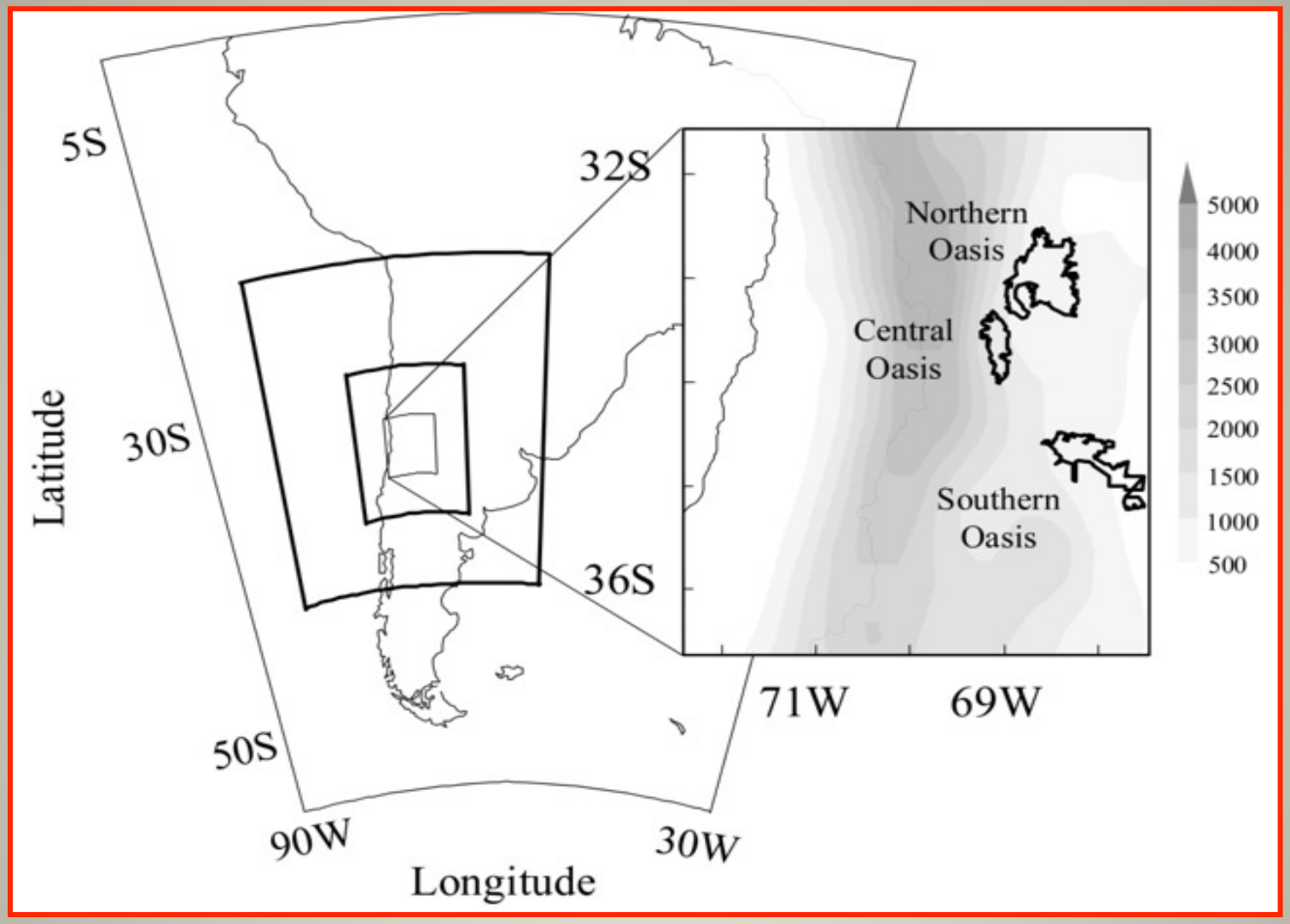

WRF: Three nested domains. Horizontal resolutions: 36 km (2500x2500 km extent), 12 km (1044x1080 km extent) and 4 km (456x564 km extent) respectively

a) and b) *w* structures corresponding to the storms on 26 Feb 2006 and 17 Mar 2010, at FRE times: 21:13 and 20:40 UT

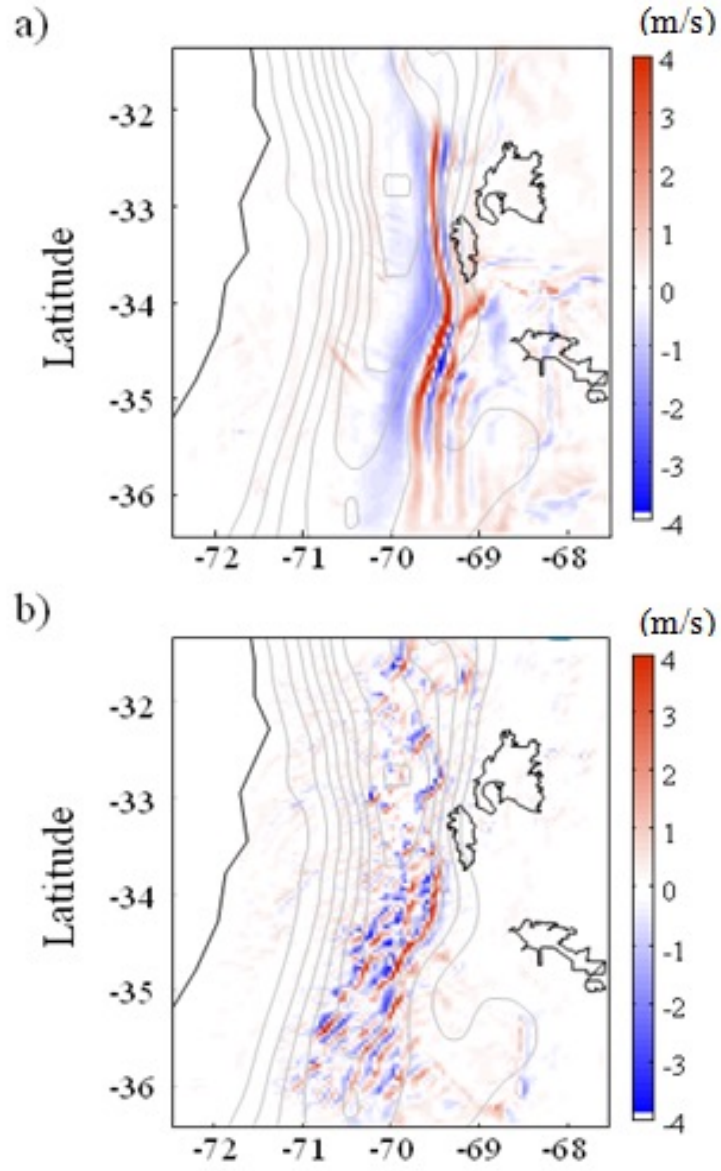

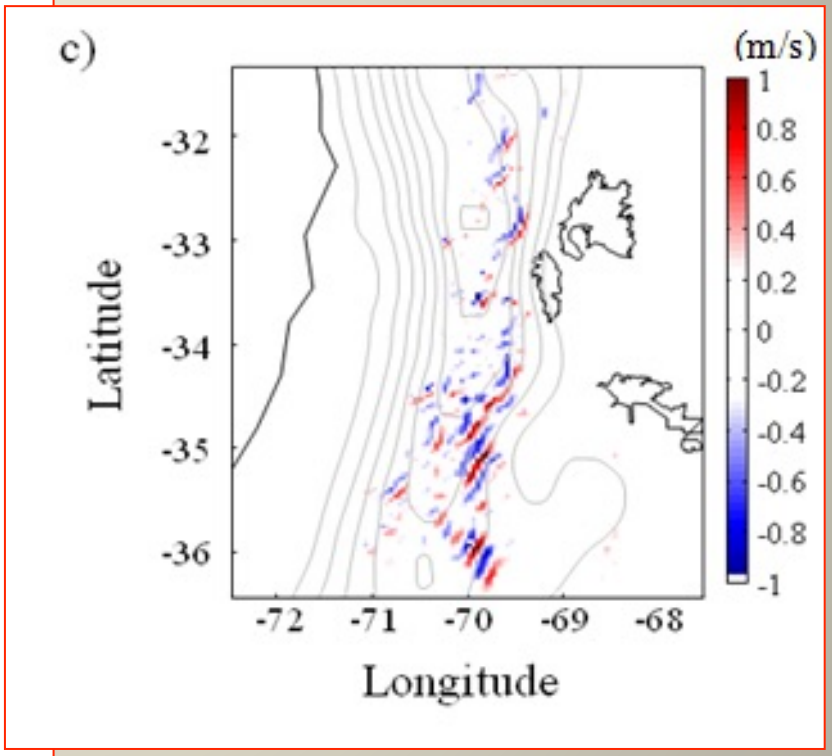

vertical velocity

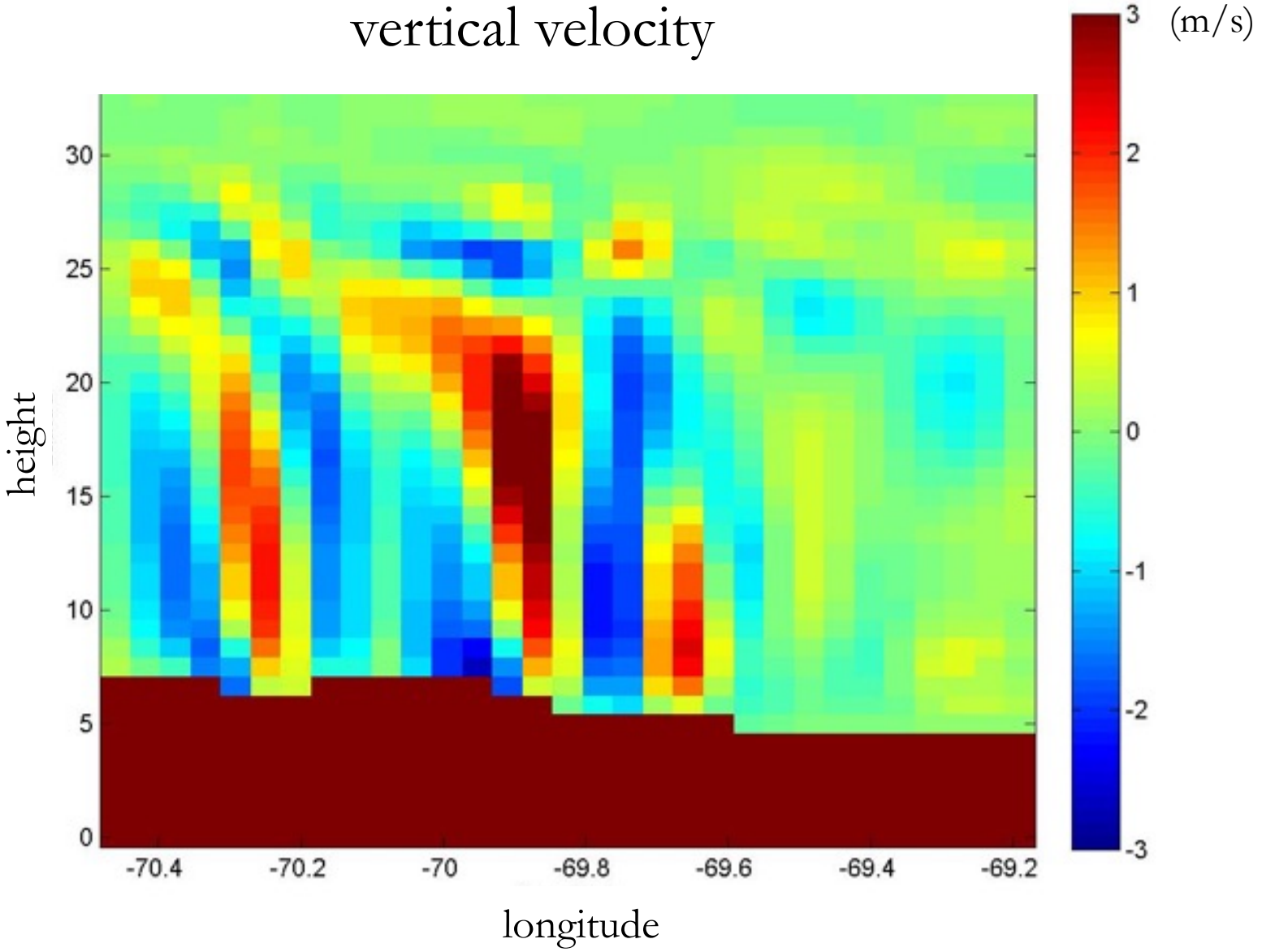

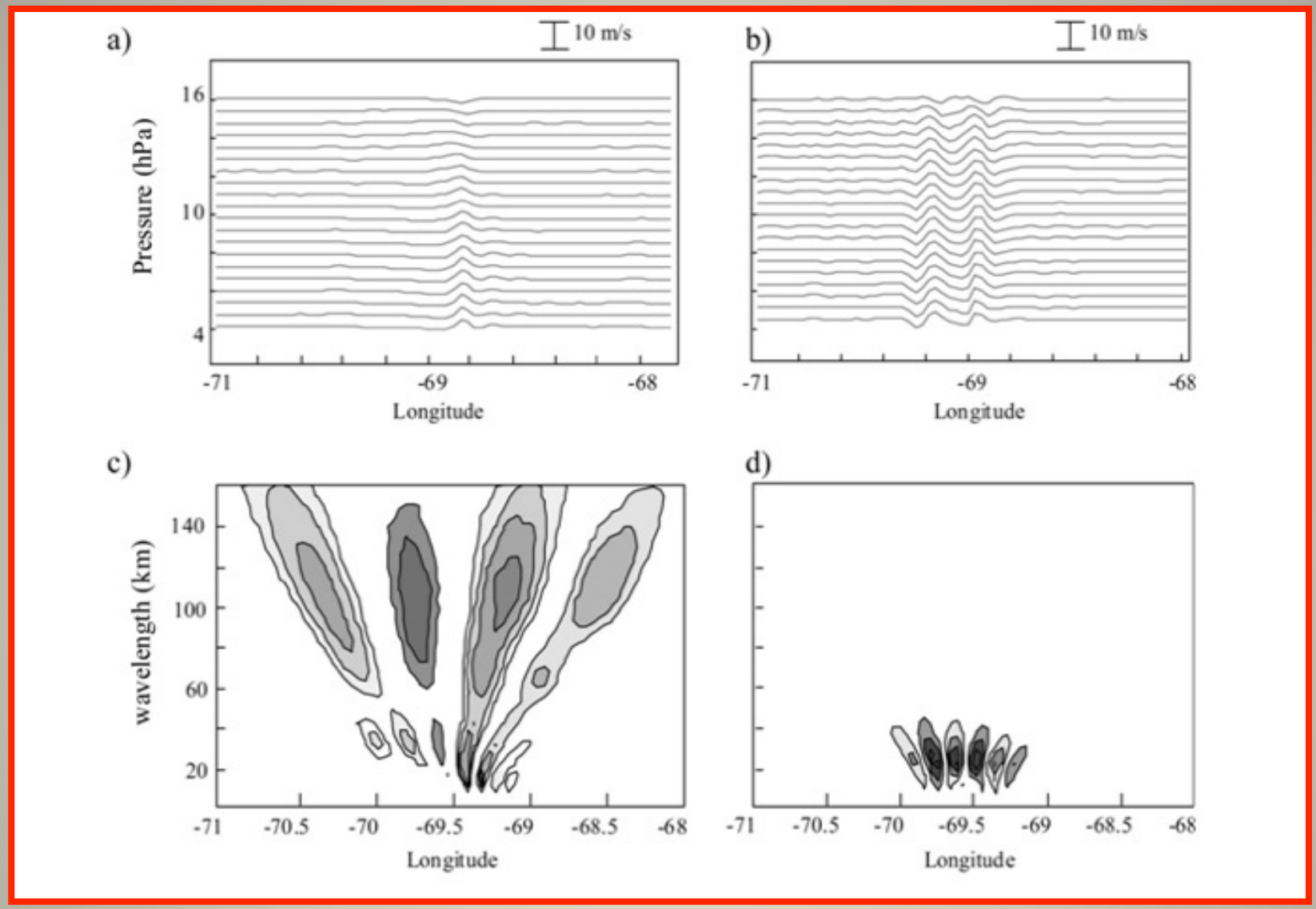

a)- b) Band-pass filtered *w* zonal profiles (ZPs) for several constant pressure levels, at latitudes coincident with FRE during C1 and C2.

c) - d) Morlet CWT from *w* ZPs at 600 hPa

$$CAPE = \int_{LFC}^{NBL} g \frac{T_{V(par)} - T_{V(env)}}{T_{V(env)}} dz$$

$$CIN = \int_{ILL}^{LFC} g \frac{T_{V(par)} - T_{V(env)}}{T_{V(env)}} dz.$$

CAPE represents the energy available to lift air parcels

CIN describes a stable surface layer, which rising air parcels have to overcome to reach the unstable layer

T_V(par, env) are the virtual temperature of the selected parcel and environment, respectively.

T_V of a moist air parcel is the temperature at which a theoretical dry air parcel would have a total pressure and density equal to the moist parcel of air.

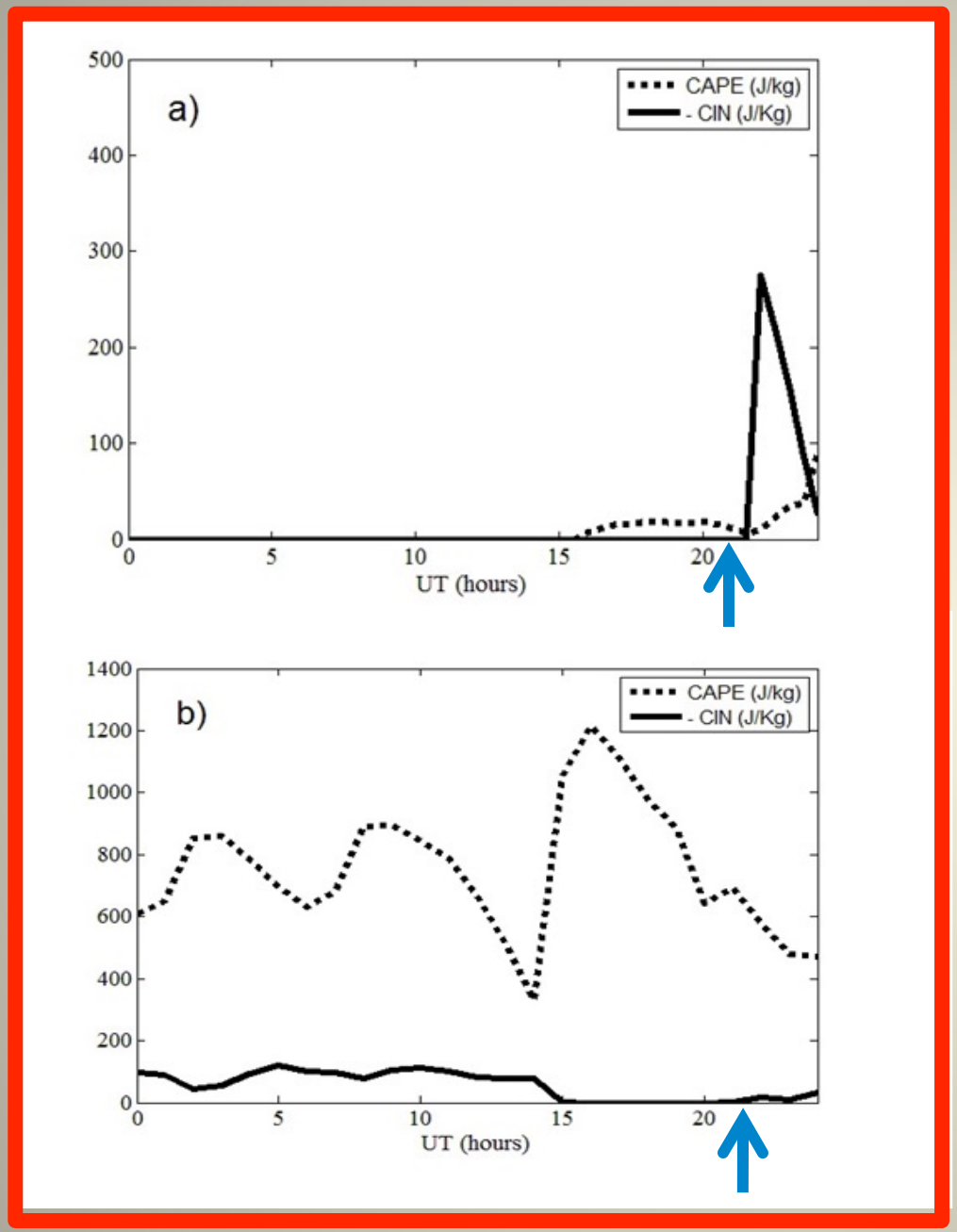

- *CIN* and *CAPE* diurnal variability, for C1 (a) and C2 (b), at the latitudes corresponding to detected FRE positions

First echo and maximum development

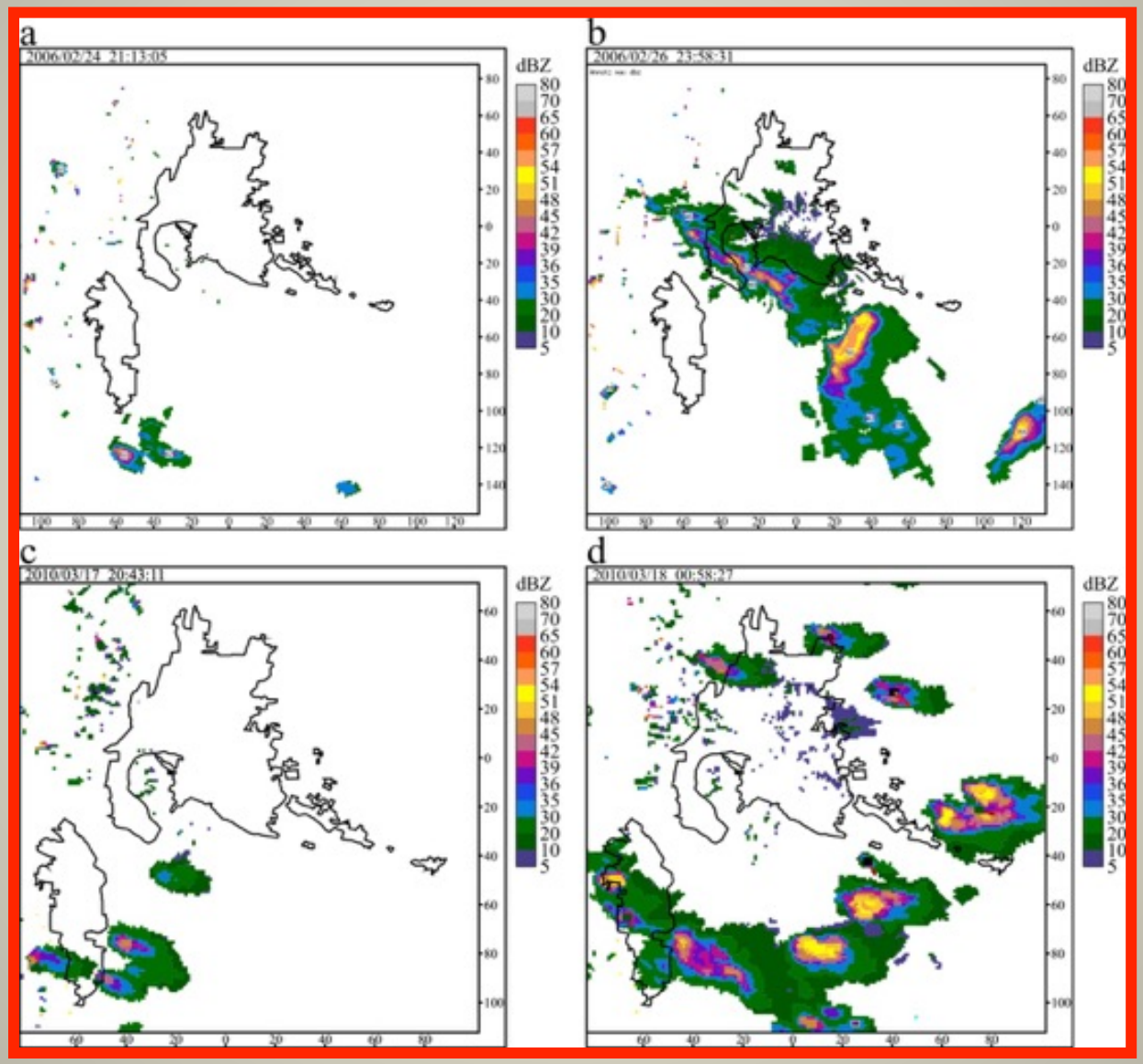

C1

C2

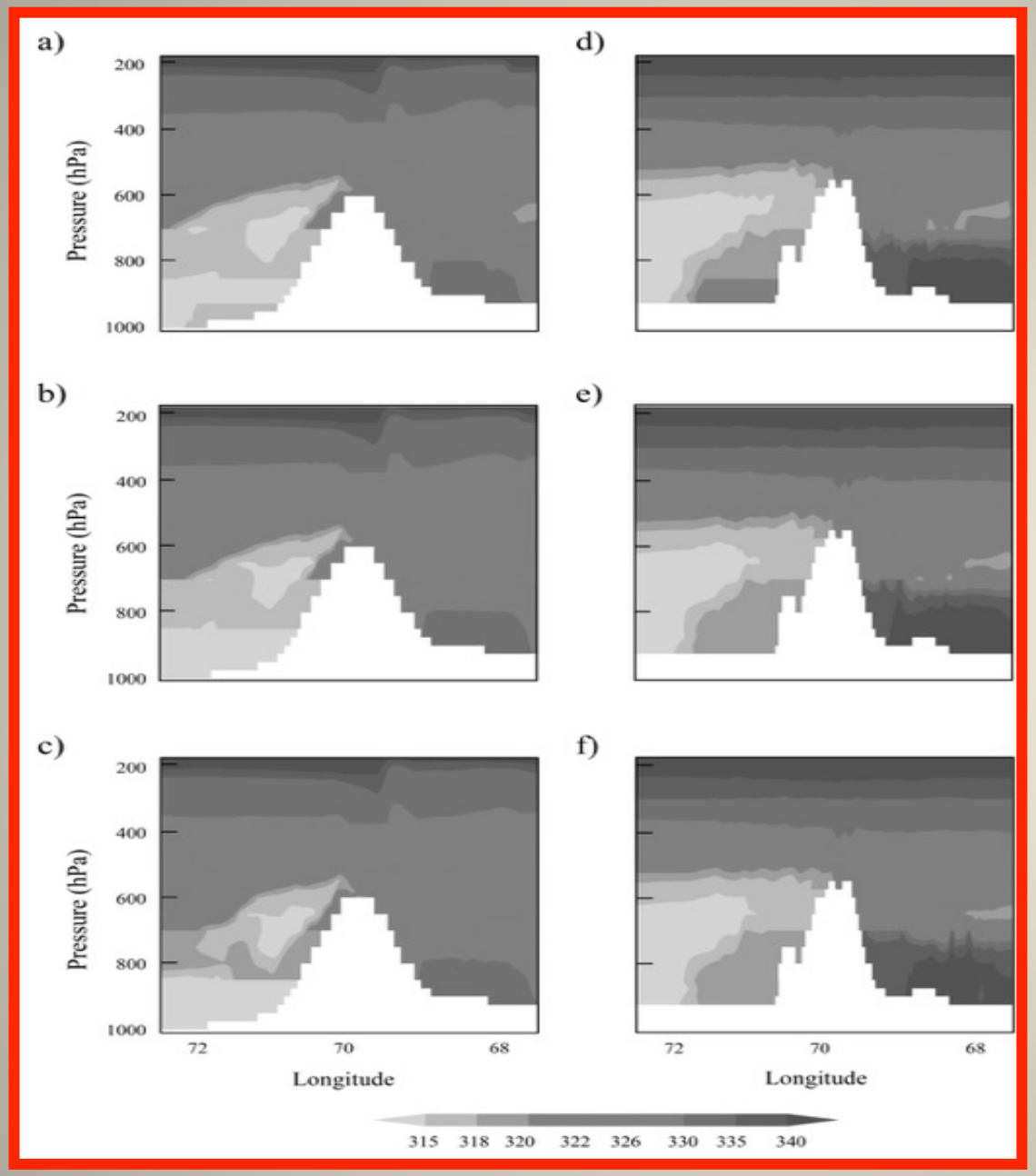

- Time evolution of equivalent potential temperature (θ_E) as a longitude-altitude presentation, at FRE latitude and a) 2, b) 1 and c) 0 hours before FRE time (C1).
- d) to f) the same, for C2.

Conceptual Scheme

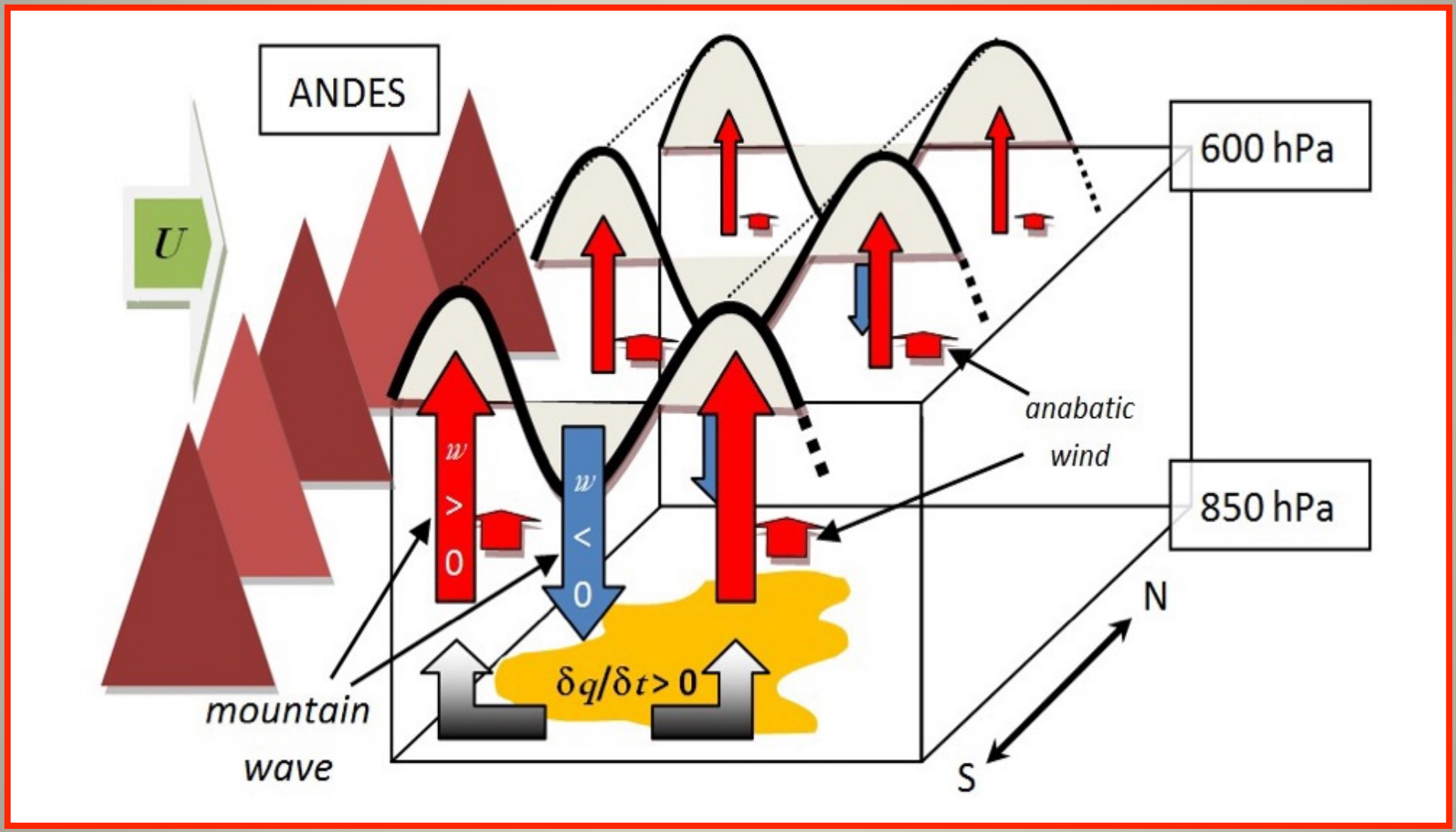

Conclusions (1.)

- **In the absence of cold fronts, after an accumulation of specific humidity and a negative vertical gradient of equivalent potential temperature at lower levels, MWs are forced at and below 600 hPa**

- **Quasi bidimensional wave structures at leeside appear above 700 hPa, with horizontal wavelengths between 25 and 30 km**

- **These structures are always found at identical locations, generating well defined and periodic positive and negative w sectors**

- **The action of anabatic winds starting in the early afternoon generates additional but much weaker updrafts above ground levels**

- **Given continuity and incompressibility conditions, a pumping mechanism driven by MWs may provide the required uplift to trigger deep convection, as far as… $1/2w^2 > |CIN|$!**

2

(Calori et al., Atmos. Res., 176–177, 267–275, 2016)

- **The tracking of humidity from other regions, previously and during the development of the storms, may be performed with the ground-based GNSS network and the integrated water vapor mapping**

- **The electromagnetic signal from a GNSS satellite suffers a delay through its pass across the neutral atmosphere, partially as result of the presence of WV**

- **45 days during midsummer**

- **SIRGAS-CON: Retrieval of integrated water vapor (IWV) content, mapping this variable by the use of a digital model of terrain**

- **Prevailing influx of humidity from N and NE and a high correlation between the accumulation/depletion of humidity and the hail/no hail precipitation days**

- **Development of five storms detected by a S-Band radar network**

- **Although the results strongly suggest that IWV maps are capable to represent the humidity dynamics in the considered region, it is still important to highlight that the calculated values for IWV are unrealistic at some locations as the consequence of deep atmospheric gradients**

- **These biases may be explained by the fact that the GNSS observations are made over the whole horizon of each given site**

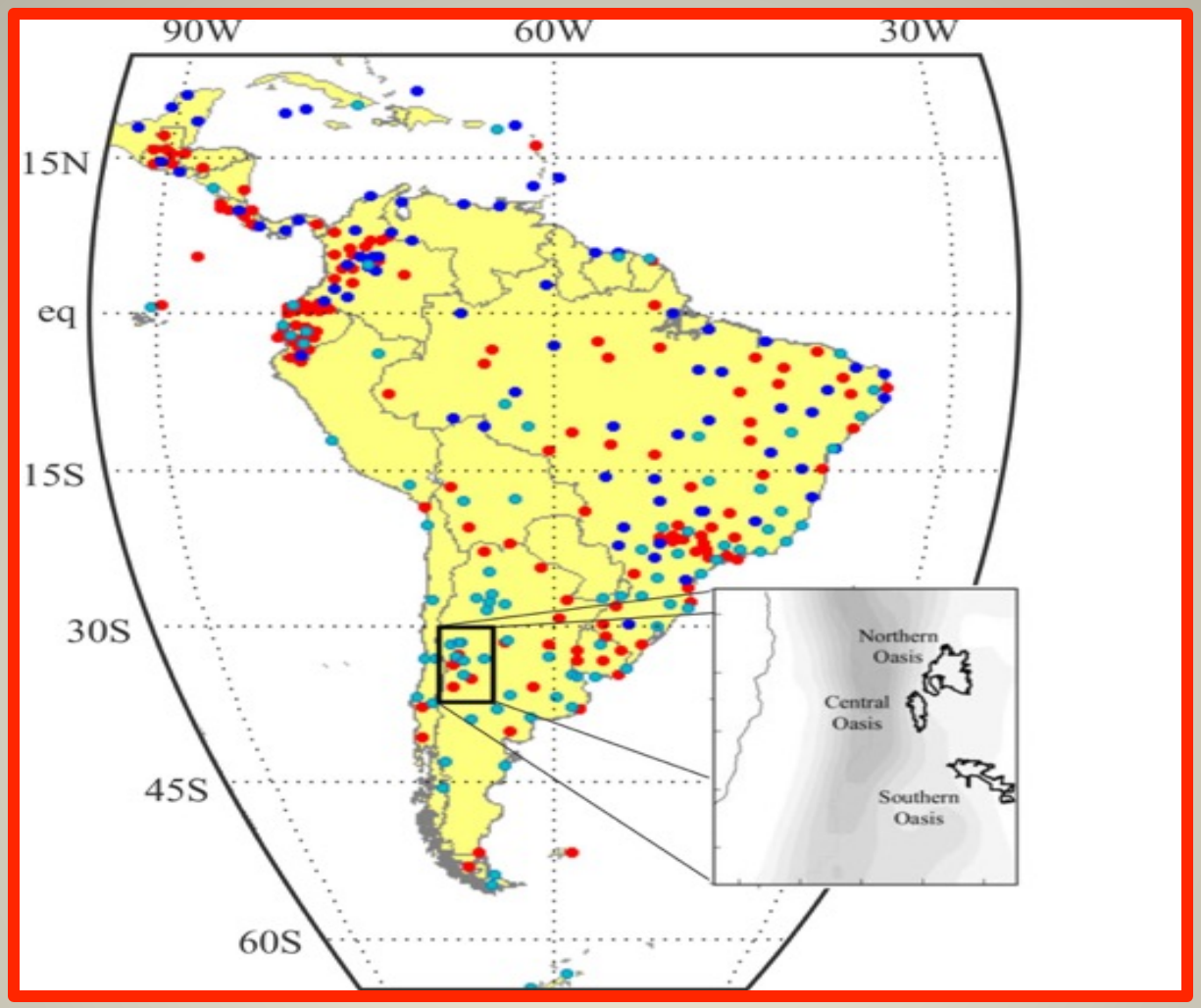

a) The SIRGAS-CON network distribution (in cian dots the SIRGAS-CON-D Sur sites, in red dots the rest of SIRGAS network at march 2010, blue dots the new SIRGAS sites from 2010 until nowadays). Black box: the Cuyo region. b) The protected oases.

Model

ZTD =ZHD + ZWD

$$ZHD = 0.0022768\left(\frac{p}{1-0.00266\cos(2\varnothing)-0.00028\,h.}\right)$$

p and T from a numerical model

$$p = SLP(1-0.000226\,h)^{5.225}$$

$$T_m = 50.4 + 0.789\,T$$

$$\Pi = 10^{-6}\left(K'_2 + \frac{K_3}{T_m}\right)R_W$$

$$IWV = \Pi.ZWD$$

a regular data grid of 0.125° is defined. Using the thin-plate smoothing spline interpolation, IWV at each grid node is computed

$$IWV_{Corr} = IWV_{Orig.}\ e^{-(HDG)/q}$$

Height Difference Grid

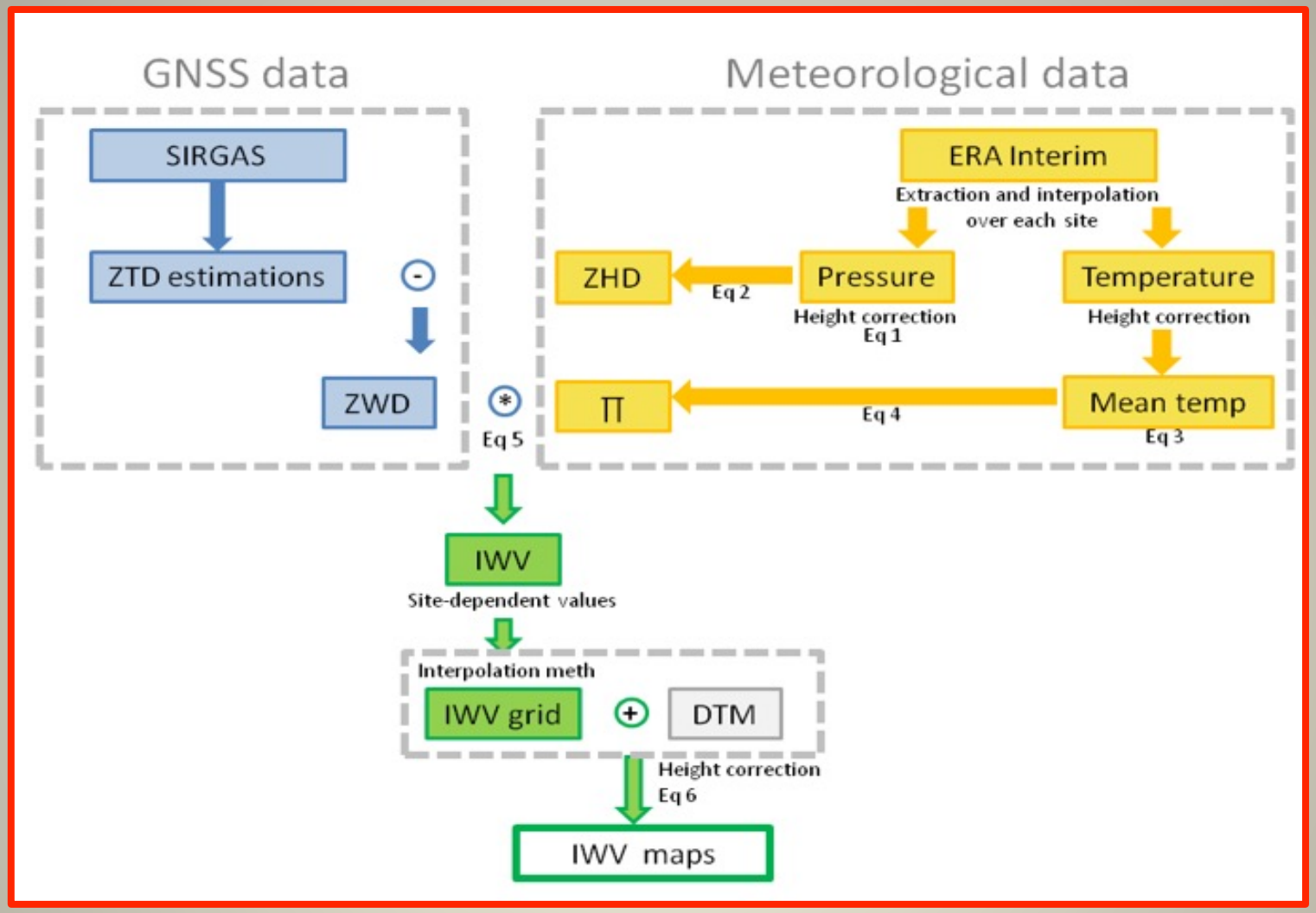

The process for IWV retrieving and mapping

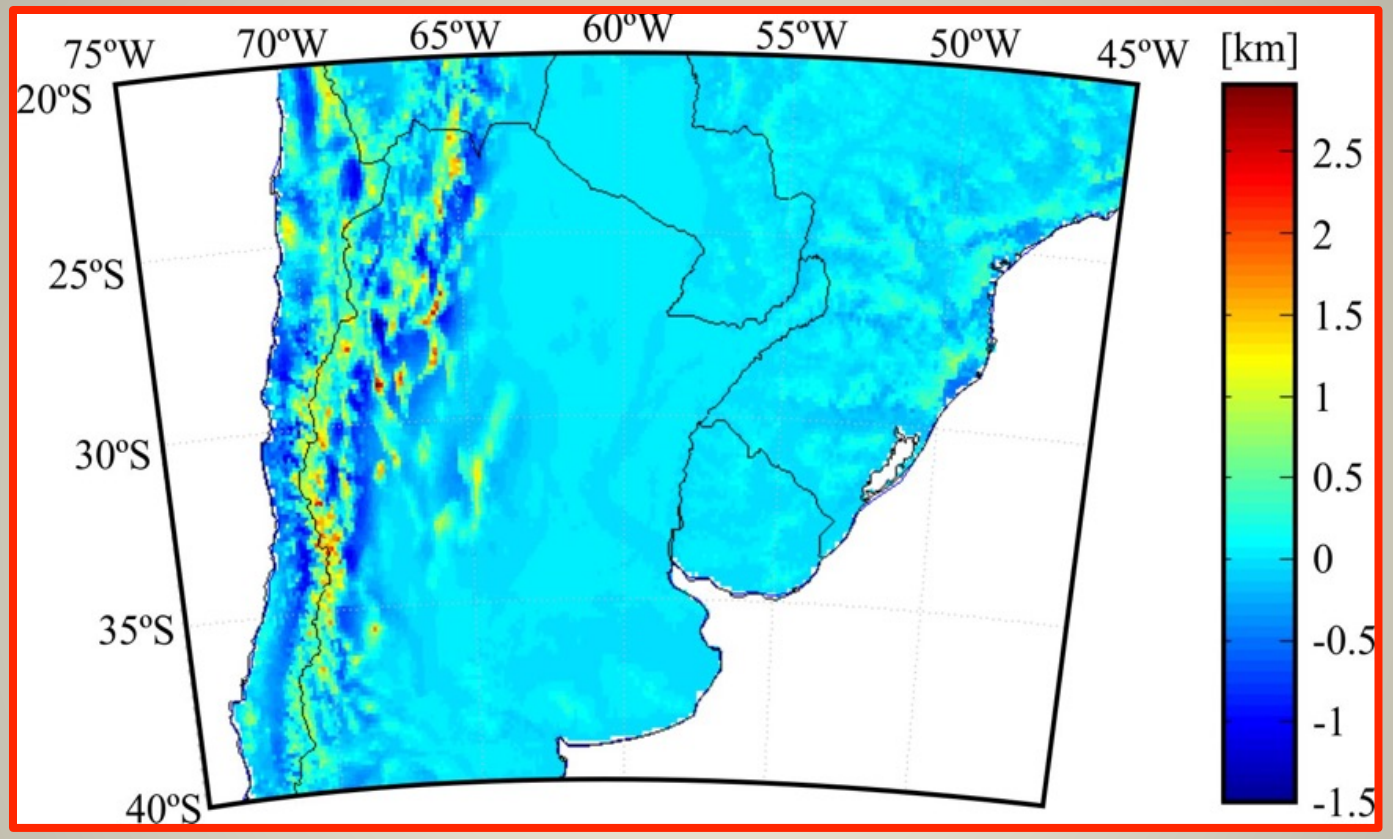

Altitude differences between ERA Interim and DEM (Digital Elevation Model)(in km)

Let us see the IWV results during one week of observations:

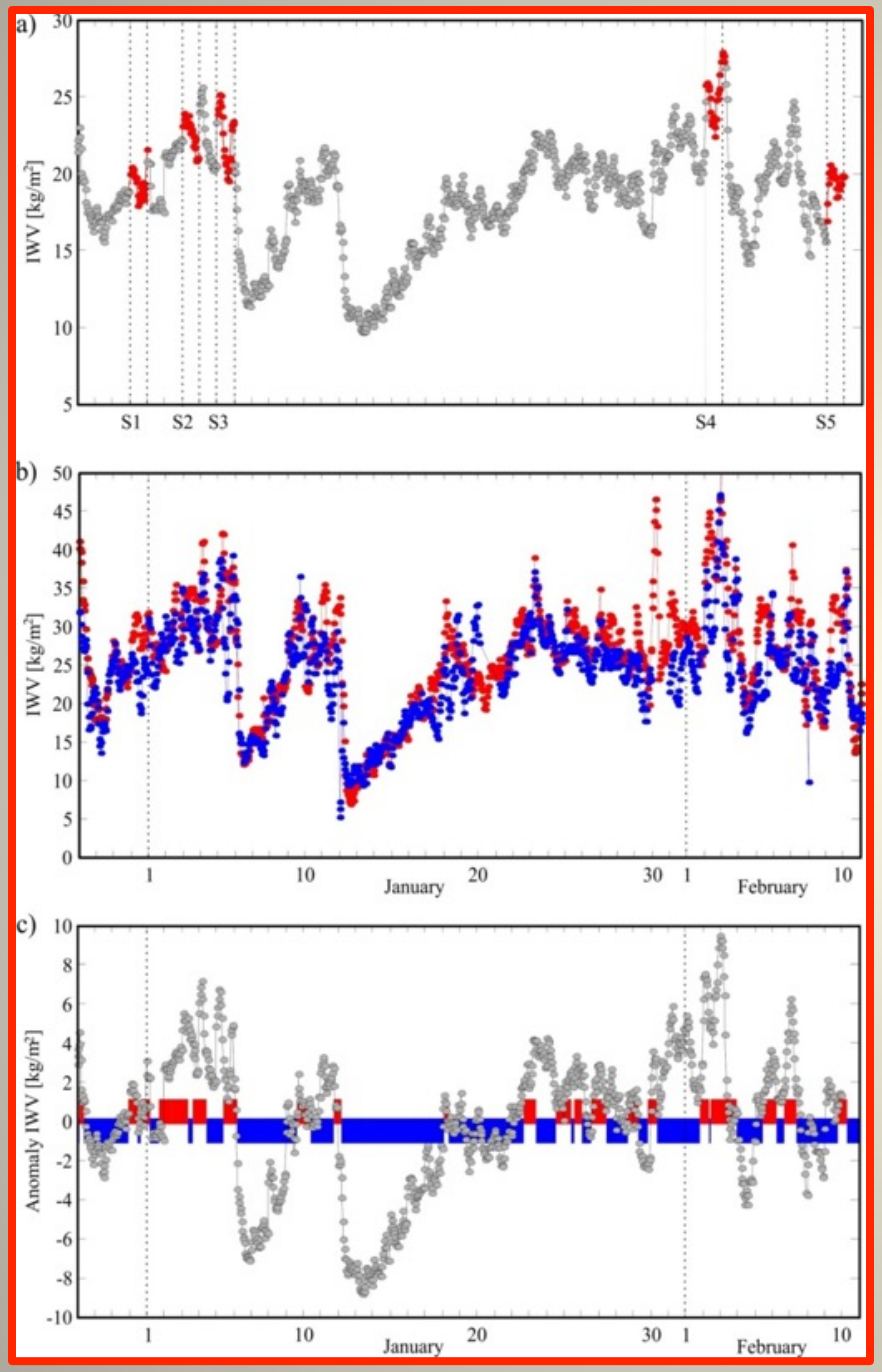

a) The variability of IWV at the interpolated mesh point located at 33.4 S, 69.1 W, and altitude = 1000 m. This point was optimally selected close enough to the typical genesis locations above the central oasis.

b) IWV as measured by the two closest GPS stations to the selected mesh point belonging to the SIRGAS network: MZAC and MZAE, in red and blue, respectively

c) IWV anomalies, after subtracting the mean value. Hail (red) and no hail (blue) precipitation days.

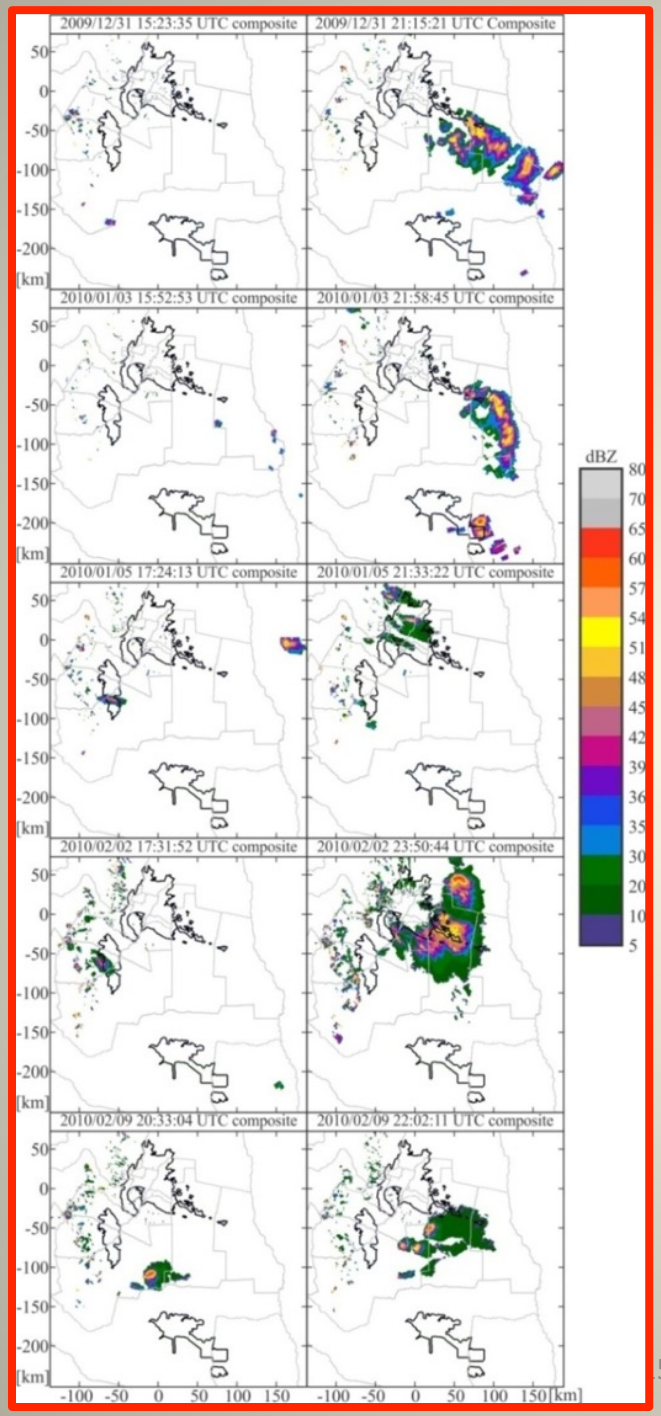

- First S-Band radar echoes (left) and maximum development (right), from top to bottom respectively, corresponding to the 5 convection events already highlighted in red color in the previous figure

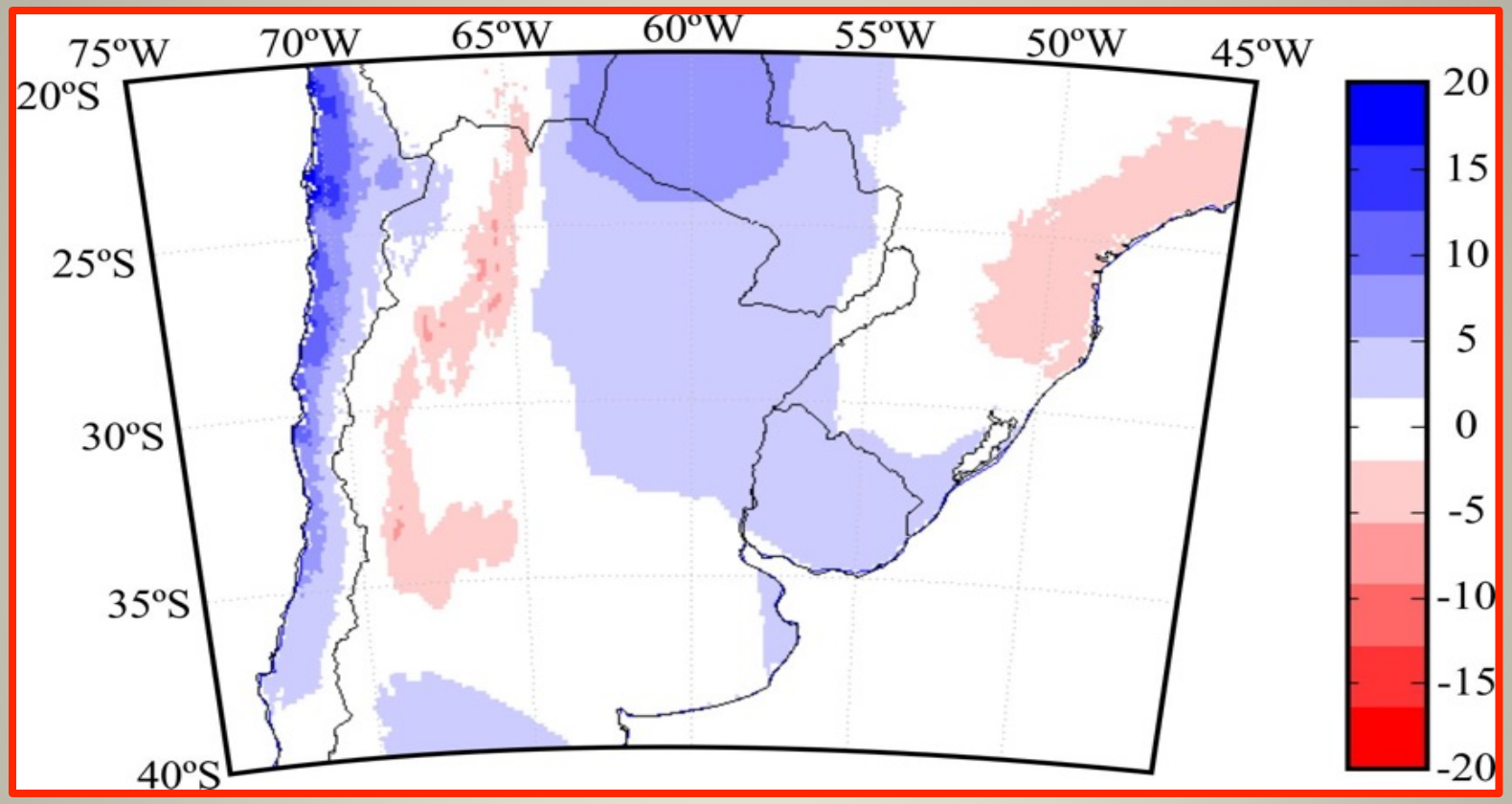

Average bias for *IWV*, in kg/m^{-2}, between the method here applied and ERA-Interim reanalyses, from the 45-days period considered

Conclusions (2.)

- **A method to observe the IWV evolution during a sequence of severe convective storms above a given geographic region of interest, in this case, the Cuyo region**

- **The constraints and hypotheses involved within the above mentioned equations may be a matter of discussion and possible improvement**

- **We believe that the potential utility of the method itself may be appreciated through these preliminary results, supported by both radar data and surface damage reports**

- **These results justify a more detailed analysis in the future, considering a longer period including several years of storm data. From the encouraging correlation observed between damage data at surface level and IWV variability, we may study the seasonal and monthly variability of this correlation**

Conclusions (2. –cont-)

- In this context, an insight of the relative importance at this region of IWV accumulation, possible triggering factors and local instability conditions (usually quantified through the CAPE and CIN indexes) may be relevant

- The five events exhibiting similar synoptic conditions were selected just to illustrate the method and were grouped by the presumed influence of the orography as the main triggering mechanism

- The SIRGAS-CON network is continuously increasing and the reliability of the results regarding IWV variability too. An improved knowledge of the optimum density of stations to study these mesoscale atmospheric events, or even to forecast them on a real-time is pending

Conclusions (2. –cont-)

- In some regions, as for example the north of Chile (Desert of Atacama), calculated values for IWV are unrealistic. This may be seen in the figure, where the average bias for IWV between ERA-Interim reanalyses and the method here applied are plotted for the considered period of study. These biases may be explained by the fact that the GNSS observation is always made over the whole horizon of a given site. In locations very close to a very large atmospheric T gradient, the GNSS technique, through the method followed to obtain ZTD in this work, is not capable to provide correct atmospheric information over this specific site

- Besides this circumscribed limitation, the GNSS meteorology is promising for monitoring severe weather events. At present, several researchers (e.g. Guerova et al., 2013) are developing and improving the methodologies for retrieval and modelling IWV from ground based GNSS networks


¡ ..y muchas gracias !